The Influence of Altered Precipitation Frequency on Biological Soil Crust Bacterial Community Structure, Diversity, and Ecosystem Functions

by

Natalie Kristine Myers

A Thesis Presented in Partial Fulfillment
of the Requirements for the Degree
Master of Science

Approved May 2013 by the
Graduate Supervisory Committee:

Ferran Garcia-Pichel, Chair
Sharon Hall
Rosa Krajmalnik-Brown
Benjamin Turner

ARIZONA STATE UNIVERSITY

August 2013

ABSTRACT

Biological soil crusts (BSCs), topsoil microbial assemblages typical of arid land ecosystems, provide essential ecosystem services such as soil fertilization and stabilization against erosion. Cyanobacteria and lichens, sometimes mosses, drive BSC as primary producers, but metabolic activity is restricted to periods of hydration associated with precipitation. Climate models for the SW United States predict changes in precipitation frequency as a major outcome of global warming, even if models differ on the sign and magnitude of the change. BSC organisms are clearly well adapted to withstand desiccation and prolonged drought, but it is unknown if and how an alteration of the precipitation frequency may impact community composition, diversity, and ecosystem functions. To test this, we set up a BSC microcosm experiment with variable precipitation frequency treatments using a local, cyanobacteria-dominated, early-succession BSC maintained under controlled conditions in a greenhouse. Precipitation pulse size was kept constant but 11 different drought intervals were imposed, ranging between 416 to 3 days, during a period of 416 days. At the end of the experiments, bacterial community composition was analyzed by pyrosequencing of the 16s rRNA genes in the community, and a battery of functional assays were used to evaluate carbon and nitrogen cycling potentials. While changes in community composition were neither marked nor consistent at the Phylum level, there was a significant trend of decreased diversity with increasing precipitation frequency, and we detected particular bacterial phylotypes that responded to the frequency of precipitation in a consistent manner (either positively or negatively). A significant trend of increased respiration with increasingly

long drought period was detected, but BSC could recover quickly from this effect. Gross photosynthesis, nitrification and denitrification remained essentially impervious to treatment. These results are consistent with the notion that BSC community structure adjustments sufficed to provide significant functional resilience, and allow us to predict that future alterations in precipitation frequency are unlikely to result in severe impacts to BSC biology or ecological relevance.

TABLE OF CONTENTS

Page

LIST OF TABLES

LIST OF FIGURES

Introduction

Desert biological soil crusts (BSCs) are cemented organo-mineral matrices that occur on the surface of many desert soils throughout the world and play important roles in desert soil ecosystem functions such as carbon and nitrogen sequestration and cycling. Primary producers such as cyanobacteria, algae, bryophytes, and lichens typically dominate the community and, in addition to their inherent carbon fixation capacities, some taxa, primarily heterocystous cyanobacteria, are also capable of fixing atmospheric nitrogen (Evans and Lange, 2003). The production of photosynthate and various nutrient acquisition strategies are essential to supporting the associated heterotrophic community that is predominantly comprised of fungi, Actinobacteria, and other heterotrophic prokaryotes (Nagy et al., 2005; Bates and Garcia-Pichel, 2009). Nutrients fixed and transformed therein can be translocated and play a significant part in supplementing nearby plant communities (Belnap, 2003a). Beyond their functions in nutrient cycling, BSCs also play important roles in desert soil integrity and structure through: 1) stabilizing mineral substrate thereby mitigating erosive forces (Belnap, 2003b) and 2) altering the surface and subsurface, influencing water infiltration and run-off (Warren, 2003).

BSCs differ from other soil types in that they possess a relatively low number of dominant taxa, relatively low diversity with regard to both species richness and evenness, and large microbial populations responsible for primary productivity (Nagy et al., 2005; Gundlapally and Garcia-Pichel, 2006; Abed et al., 2012). For these reasons, BSCs have been proposed as a model system for studying biodiversity-ecosystem function relationships in soils (Bowker et al., 2010). Due to low taxonomic diversity in BSCs and

potentially low functional redundancy, shifts in community structure and any resulting functional changes may be more pronounced. Previous studies have shown that the metabolic activity time in a BSC is limited by the amount of precipitation received and the rate of evaporation that follows (Garcia-Pichel and Belnap, 1996; Belnap, 2003c), but it is not well understood how or even if precipitation *frequency* is responsible for shaping BSC community composition, diversity, and associated ecosystem functions. This topic was first addressed from a functional perspective in a precipitation frequency alteration study in BSCs (Belnap et al., 2004). Small precipitation pulse sizes resulted in the attenuation of net photosynthetic carbon gains, i.e. carbon deficit, due to the inability of the BSC to restore photosynthesis prior to desiccation. It is difficult to accurately determine which was the more impactful variable, precipitation frequency or precipitation pulse size; bacterial community composition and diversity were not analyzed. In a similar multi-year altered precipitation frequency study dramatic carbon deficits were demonstrated, and yet complementary molecular analysis showed no detectable bacterial community composition changes at the phylum level (Johnson et al., 2012). A survey-type study of BSCs across seven biomes in southern Africa, however, implicated precipitation frequency and not mean annual rainfall (MAR) as the major driver of BSC community composition, diversity, and succession (Evans and Lange, 2003; Büdel et al., 2008). The present study provided the opportunity to parse the influences of precipitation frequency from those of precipitation pulse size by treating a single soil type, replete with the same inherent BSC community, in a controlled setting with unaltered precipitation pulse size.

The potential influence of precipitation frequency on BSC composition and ecosystem functions is especially relevant within the context of projected climate change for the arid and semi-arid climates of the southwestern United States. The general climate change pattern predicted for the region is a hotter, drier climate that could even outpace more mesic climates in North America in its rate of warming (Nagy et al., 2005; Weiss and Overpeck, 2005; Christensen, 2007; Bates and Garcia-Pichel, 2009; Overpeck and Udall, 2010). The Sonoran desert in particular is semi-arid, receiving 75-300 mm of rain per year, and its precipitation regime is characterized by two seasons that produce the year's most significant rainfalls: the summer monsoon season in July-August and winter storm systems that occur in Dec-Feb (Rosentreter and Belnap, 2003; Belnap, 2003a). The monsoon rains are spatially isolated with small pulse sizes (<5 mm) while winter storms are often more ubiquitous in coverage and may deliver precipitation pulse sizes in excess of 20 mm. Climate change predictions specific to precipitation in the Sonoran desert region are somewhat confounding, however. While most models predict reduced winter precipitation as a result of more northerly winter storm tracks, the behavior of the summer monsoon is more difficult to accurately predict. Historic climate data reveals that past warming in the Sonoran desert has resulted in both increased and decreased precipitation levels associated with the monsoons and current predictive computer modeling is in agreement with this scenario (Belnap, 2003b; Christensen, 2007; Seager et al., 2007; Cook et al., 2010). Regardless of warming, it is possible that varied intensity of the monsoon could result in longer or shorter intervals of drought throughout the year. Unlike many soils that retain some level of bio-available water content between precipitation events, BSCs in the Sonoran desert are subjected to near or complete drying

between rains (Warren, 2003; Belnap, 2003c). The stresses associated with prolonged desiccation and reactivation upon wetting could variably influence BSC bacterial populations that possess different physiological strategies to cope with desiccation and rewetting (Potts, 1994; Fierer and Schimel, 2002; Nagy et al., 2005; Gundlapally and Garcia-Pichel, 2006; Abed et al., 2012), potentially altering the community composition, diversity, and related ecosystem functions.

Many biotic and abiotic factors have been evaluated for their potential in shaping microbial community structure and diversity in a variety of soil types (Fierer and Jackson, 2006; Lauber et al., 2009; Bowker et al., 2010; Fierer et al., 2011). While several variables such as precipitation, elevation, and latitude have long been identified as good predictors of animal and plant diversity, the same cannot be projected for microbial biota in soils (Garcia-Pichel and Belnap, 1996; Belnap, 2003c; Fierer et al., 2011). Many studies have examined the influences of temperature, parent material, precipitation, land use type, and latitude on soil community composition and diversity (Belnap et al., 2004; Acosta-Martínez et al., 2008; Rivera-Aguilar et al., 2009; Bachar et al., 2010) but no strong correlations have materialized with regards to those factors. In the last decade, however, pH has emerged as one of the strongest drivers, if not the most important, in shaping overall bacterial community composition and diversity in soils (Fierer and Jackson, 2006; Lauber et al., 2009; Johnson et al., 2012). pH has not been exclusively examined in BSCs for its potential in shaping the microbial community but related investigations have identified some trends in community composition, diversity, function, or taxon occurrence correlated with temperature, precipitation, pH, and/or latitude (Belnap, 2003c)(Garcia-Pichel et. al. in review). Most of these studies, however, have

emphasized either 1) community composition and diversity as influenced by the factor(s) analyzed or 2) ecosystem functions as influenced by the factor(s) analyzed.

In the present study, we used an experimental rather than a correlational approach to look at the effects of precipitation frequency. We examined the influences of a long-term precipitation treatment on early- to mid-succession BSCs using high-resolution molecular analyses of the bacterial community complemented by functional community assays to probe for any accompanying changes in carbon and nitrogen cycling. Intact BSCs from the Sonoran desert were used to establish microcosms that were subjected to altered precipitation frequencies below, within, and above the range experienced *in situ*. The treatment at the lowest end of the precipitation gradient (0 days/yr) was not wetted for the duration of the study (416 days) and the treatment at the highest end of the precipitation gradient was wetted every 3 days (120 days/yr). The precipitation pulse size was constant (10 mm), meaning the MAR scaled with the precipitation frequency (ex. 120 days/yr = 1200 mm MAR). Despite temperature fluxes through the seasons, all microcosms desiccated to a minimum of 99.5% of the precipitation volume between each wetting event. We predicted that bacterial species richness, diversity, and functional diversity would (1) peak in/near the middle of the precipitation gradient at an optimal precipitation frequency (2) decline with reduced precipitation frequency as a function of cellular degradation and failure to reanimate and (3) decline with increased precipitation frequency as a function of reduced water stresses and increased competition. We also expected that after the treatment, certain microbial taxa would be enriched in the different treatments, thus revealing any niche partitioning regarding frequency of precipitation in crust biota.

Experimental Procedures

Field Site & Sampling Approach

Early successional biological soil crust (BSC) samples were collected in the Sonoran Desert in May 2010 near Casa Grande, Arizona (32° 59' 28.9" N, 111° 45' 40.6" W). The landscape was primarily dominated by creosote shrub (*Larrea tridentata*), some small cactus species, and sparse grass stands (Figure 1c). Close inspection of the interplant BSCs revealed small black colonies of free-living *Nostoc sp.*, scattered *Collema sp.* lichen (with *Nostoc sp.* as photobiont); greening and the appeareance of *Microcoleus sp.* bundles of filaments was observed upon wetting. BSCs were excised from the ground using stainless steel frames and placed in polycarbonate containers according to the procedure described in Supplementary Data Figure 1.

Microcosm Setup & Precipitation Treatment

The polycarbonate containers housing the BSC samples (or microcosm "pots") were incubated for the duration of the 416-day treatment in a rooftop greenhouse at Arizona State University in Tempe, Arizona (Figure 1a) from July 2010 to September 2011. *In situ* climate conditions were mimicked by leaving the greenhouse aeration open to the outside and shutting off temperature control. The microcosms were shielded from natural precipitation. Stand fans were placed at each end of the bench housing the microcosm setup to provide consistent air flow over the samples. Each microcosm pot was submitted to one of 11 different watering treatments corresponding to precipitation frequencies of 0, 1, 2, 4, 8, 16, 32, 60, 80, 100, and 120 days (events) per year. Treatments are referred to as "0, 1, 2, 4, 8, 16, 32, 60, 80, 100, and 120" from here forward. Three microcosm replicates were set up for each treatment. Each precipitation

event occurred at 9 a.m. (prior to intense, overhead sunlight) and consisted of the automatic delivery of 200 mL ddH_2O by a high-pressure misting system on timers (equivalent to a 10 mm precipitation event by surface area). All analyses were performed after the completion of the treatment.

Nucleic acid extraction and purification

Cell lysis and total nucleic acid extraction was performed essentially as described by (Garcia-Pichel et al., 2001) with some modifications. Microcosm pots were sampled (Table 1, B) and 0.5 g BSC homogenate from each of three replicate pots in a treatment was combined, totaling 1.5 g, and represented a composite of the treatment. Briefly, 1.5 g BSC homogenate was suspended in 3.75 mL TESC buffer (100mM Tris-HCl pH 8, 100mM EDTA, 1.5M NaCl, 1% (wt/vol) CTAB) with 2.25 g zirconia/silica beads (.5 mm). The soil/bead mixture was subjected to 3 freeze/thaw cycles in liquid nitrogen. SDS was added to a final concentration of 1% (w/v) and proteinase K was added to a final concentration of 100 μg/mL. The sample was incubated for 30 minutes at 50°C. Cells were mechanically lysed by vortexing and the lysate cleared by centrifugation. Cleared lysate was subjected to two P:C:I (phenol:chloroform:isoamyl alcohol; 25:24:1) extractions (1:1 vol) followed by two C:I (chloroform:isoamyl alcohol; 24:1) extractions (1:1 vol). Nucleic acids were precipitated by the addition of 3 M sodium acetate (final concentration 0.3 M) and ice-cold absolute (100%) ethanol (final concentration 70%) and incubated at -80°C for 24 hours. Nucleic acids were pelleted by centrifugation at 13,000 x *g* at 4°C for 30 minutes and washed once with 70% ethanol. The pellet was air-dried and then suspended in TE buffer (10mM Tris-HCl, 1 mM EDTA at pH 8). Nucleic acids were checked for quality and concentration on a 1% agarose gel.

Due to the presence of brown-colored clays and/or humics complexed with the purified nucleic acids, it was necessary to further purify the DNA prior to downstream applications (PCR was inhibited when the brown-colored extract was used as template). The Mo-Bio PowerClean® DNA Clean-Up Kit was used to purify 100uL of the brown extract (~20% of the total extraction) according to the manufacturer's protocol. The resulting DNA eluent was checked for quality and concentration on a 1% agarose gel. Samples were stored at -20°C until processed.

PCR and pyrosequencing

Purified community DNA was submitted to Molecular Research LP (Shallowater, Texas) for 16S rRNA gene amplification and subsequent sequencing on a 454 Roche pyrosequencer. Bacterial 16S rRNA genes were amplified using the forward primer 530F 3'- GTGCCAGCMGCNGCGG 5' and the reverse primer 1100R GGGTTNCGNTCGTTR, effectively covering hypervariable regions IV, V, and VI. A single-step 30-cycle PCR was performed using HotStarTaq Plus Master Mix Kit (Qiagen, Valencia, CA). The cycling conditions were 94°C for 3 minutes, 28 cycles (94°C for 30 secs; 53°C for 40 secs; 72°C for 1 min), and a final elongation step at 72°C for 5 minutes. Following PCR, all amplicon products from different samples were mixed in equal concentrations and purified using Agencourt Ampure beads (Agencourt Bioscience Corporation, MA, USA). Samples were sequenced utilizing Roche 454 FLX titanium instruments and reagents according to manufacturer's guidelines.

Analysis of bacterial 16S rRNA gene sequences

16S rRNA gene sequence reads generated by the Roche 454 sequencer were processed using the Quantitative Insights Into Microbial Ecology (QIIME, specifically

MacQIIME v1.5.0) (Caporaso, Kuczynski, et al., 2010) pipeline as previously described (Gilbert et al., 2012). In the first trimming and quality-filtering step, primer and barcode sequences were removed and filtered based on length (minimum sequence length, 200 base pairs), quality (minimum average quality score allowed in read, 25), ambiguous base calls (maximum number of ambiguous nucleotides, 6), and homopolymer content (maximum length of homopolymer run, 6 nucleotides). Sequences were then clustered into Operational Taxonomic Units (OTUs) at 97% pairwise identity using the UCLUST algorithm (Edgar, 2010) and representative sequences for all OTUs were aligned to the Greengenes imputed core reference alignment (DeSantis et al., 2006) using PyNAST (Caporaso, Bittinger, et al., 2010). Taxonomy of OTU representative sequences was assigned using the internal Ribosomal Database Project (RDP) Classifier v2.2 (Wang et al., 2007). The primer set employed also amplified some (but not all) archaeal sequences; these were removed. For this, the original OTU table was split at the domain level into two tables. The Bacteria OTU table was then filtered to remove singletons and used for all downstream analyses.

After processing the sequences, the alignment was further amended for subsequent alpha diversity analyses. Chimeric sequences were identified using ChimeraSlayer (Haas et al., 2011) and excluded entirely from the working data set. The alignment was further filtered to remove gaps and hypervariable regions using a Lane mask. An approximate maximum-likelihood tree/phylogeny was constructed from the filtered alignment using FastTree (Price et al., 2010). The tree and Bacteria OTU table were used for rarefaction determination and alpha diversity analyses (OTU-based richness and Shannon-Weaver index). A total of 2295 OTUs was detected in all 11 BSC

composite samples combined. The average number of sequences per sample (sequencing effort) was 4034 but the lowest number of sequences per sample observed was 2302 (treatment 80). Sequencing effort bias was removed (rarefied) by resampling to the smallest individual sample sequencing effort (2302 sequences) for alpha diversity comparisons. The same procedures were used for alpha diversity analyses of the cyanobacterial community composition. A total of 164 cyanobacterial OTUs was observed in all 11 BSC samples combined. The average number of sequences per sample (sequencing effort) was 950 but the lowest number of sequences per sample observed was 358 (treatment 80). Cyanobacterial sequences were rarefied by resampling to the smallest individual sample sequencing effort (358 sequences) for alpha diversity comparisons.

Phylotype (OTU) survey

Whole communities in all 11 treatments were surveyed for phylum-level and phylotype-level correlations with increasing precipitation frequency (Tables 2 & 3). The Bacteria OTU table was rarefied and resulted in 2179 different OTUs overall. The rarefied OTU table was used to determine the number of OTUs in each phylum and those that comprised more than 0.5% of the sequences (i.e., common phylotypes). Under this criterion there were 109 common OTUs overall (Table 2). For every phylum represented in each treatment, OTU richness is reported as the sum of detected phylotypes and relative abundance is reported as the sum of percent community composition. To determine if the richness or representation of a particular phylum responded to treatments, we conducted linear regression and significance is reported at both $p < 0.05$ and $p < 0.1$.

pH Measurement

pH was measured using subsamples (Table 1, B) from each microcosm. Dry samples that had been stored frozen were allowed to thaw at room temperature and soil pH was measured in a 1:2 mass to volume ratio (grams dry soil:milliliters water) of Milli-Q water (EMD Millipore, Billerica, MA) with a field pH probe (SympHony SP70P, VWR).

Chlorophyll a concentrations

Chlorophyll *a* concentrations were measured for each microcosm after extraction for 24 h at 4°C in a 1:10 volume ratio of soil:90% acetone. Chlorophyll *a* concentrations were determined by absorbance at 664 nm on a UV-Visible Spectrophotometer (Shimadzu UV-1601). Areal concentrations were calculated using the original surface area of the core sample (95 mm^2) and reported in square meters.

Net photosynthesis, gross photosynthesis and dark respiration

Rates of net photosynthesis and dark respiration of intact BSCs were measured following the methods of (Strauss et al., 2012). CO_2 flux was measured under controlled conditions in the laboratory using an open infrared gas analyzer (IRGA) system (Li-COR Li-8100). A custom cylindrical stainless steel gas chamber open at one end (inner diameter 9 cm, height 2.8 cm, area 63.6 cm^2, volume 178.2 cm^3) with built-on collar (2.5 cm height) was constructed to fit inside the BSC microcosm containers. The roof of the chamber was a removable Pyrex glass petri dish bottom, fitted with a rubber gasket around the circumference of the top and effectively closed for measurement. This allowed illumination of the soil surface. The light source was a custom-built high-

powered LED (warm white 40 watts, LedEngin©) that emitted minimal infrared radiation.

BSC were wetted with 200 mL Milli-Q water (10 mm precipitation equivalent) and the custom chamber was inserted 2.5 cm deep into the crust. The BSCs were incubated under 350 μmol m^{-2} s^{-1} PAR at 25°C for 1 hour, equivalent to about the light intensity of an overcast day. Net photosynthetic rates were measured as CO_2 drawdown, three times in the light over a course of 10 minutes. Each measurement was integrated for 2 minutes with data collected every second. After the final light measurement, the light source was turned off, and the sample was placed in a dark chamber for two minutes. Dark respiration rates were measured four times in dark over a course of 14 minutes. Measurements were made for 2 minutes with data collected every second. The first measurement made in the dark revealed that the BSCs had not reached steady state so only the last three measurements made in dark were used in determination of the dark respiration rates. Gross photosynthetic rates were calculated as the difference between net photosynthetic rates and dark respiration rates and reported as positive values. After measurements, microcosms were allowed to dry, and after 15 more days a second set of measurements was carried out. This time microcosms were incubated for a full diel cycle (12 hours in dark, 12 hours under 250 μmol m^{-2} s^{-1} PAR at 30°C) in a growth chamber before the actual determinations. Immediately prior to measurement BSCs were incubated under 350 μmol m^{-2} s^{-1} PAR at 25°C for 5 minutes. Three hours was allowed for before the dark measurements in this second round. CO_2 flux was otherwise measured and reported as before.

Carbon substrate utilization

Carbon substrate utilization patterns were determined using Biolog EcoPlates™ (Biolog, Inc., Hayward, CA). 2.5 grams of BSC homogenate (Table 1, D) was added to 7.5 mL sterile Ringer's solution (25%) with sodium pyrophosphate (0.18% final concentration) and subsequently serially diluted to 10^{-2} in sterile Milli-Q water. Two Biolog EcoPlates™ were inoculated with three replicates of each treatment (32 wells per replicate; total 96 wells) by the addition of 100µL of the diluted soil suspension (10^{-2}) to the wells. In order to introduce sufficient biomass to each well, it was necessary to use a 10^{-2} dilution to inoculate the plates, which was still quite turbid. As a result, clays and silts settled in the wells and the plates could not be read with a plate reader and observations were instead made by eye. One EcoPlate™ was incubated at 30°C aerobically and the other was incubated at 30°C in an anaerobic chamber. Plates incubated aerobically were visually scored every 24 hours (for 168 hours) for the presence or absence of the purple formazan dye (indicating substrate oxidation). Plates incubated anaerobically were visually scored once after 168 hours in the anaerobic chamber.

Potential nitrogen fixation

Potential N-fixation rates were measured by the acetylene reduction assay essentially as described by (Jeffries et al., 1992). BSC microcosms were subsampled and introduced to 160mL glass bottles and wetted with autoclaved Milli-Q water to just under field capacity. The bottles were preconditioned in a growth chamber under 175 µmol m^{-2} s^{-1} PAR at 30°C for 24 hours. After preconditioning, bottles were sealed and acetylene was added to 15% (v/v) of headspace volume. Sealed bottles were incubated under 175

μmol m^{-2} s^{-1} PAR at 30°C and headspace gas was sampled at 0, 4, 8, and 24 hours and analyzed for ethylene production with a gas chromatograph (Varian 3300) equipped with a flame ionization detector and a preconditioned 6' x 1/8" SS Porapak R 80/100 column (Sigma-Aldrich/Supelco). Ethylene production was converted from nmol ethylene to μmol N using a conversion factor of 1 (Belnap, 2002). Areal N-fixation rates were determined by dividing total N production by the original area of the sample.

Ammonium oxidation rates

Potential ammonium oxidation rates were measured by the chlorate inhibition assay as previously described (Johnson et al., 2005) with some modifications. Microcosms were subsampled (Table 1, D) and 10 g BSC homogenate was slurried with 100 mL ammonium-amended nitrification potential solution (with 75 mM sodium chlorate) and incubated in the dark on a shaker at 180 rpms for 6 hours at 25°C. 10 mL aliquots were taken at 0, 2, 4, and 6 hours and cleared by the addition of 5 drops flocculant solution (7.35 g $CaCl_2$•$2H_2O$ and 10.15 g $MgCl_2$•6 H_2O in 100 ml H_2O) and centrifugation at 10,000 x *g* for 10 minutes. Cleared supernatant was filtered with pre-leached Whatman #1 filters into autoanalyzer tubes and samples were analyzed for NO_3-N accumulation using a flow-injection colorimetric autoanalyzer (Lachat Instruments, Mequon, Wisconsin). Areal rates were determined by dividing total NO_3-N accumulation by the original area of the sample.

Potential denitrification rates

Potential denitrification rates were determined with the acetylene inhibition assay as described by (Groffman and Tiedje, 1989). BSC subsamples (Table 1, E) were introduced to 160 mL crimp-top glass bottles and denitrification solution (0.72 g KNO_3 +

0.5 g glucose in 1 L Milli-Q water, pH 7.3) was added in a 1:1 ratio (soil:solution). The bottles were sealed, flushed with N_2 gas to achieve anoxia, and acetylene was added to 10% (v/v) of headspace volume. Bottles were incubated in the dark at 25°C and headspace gas samples were taken at 10 minutes and 4, 8, and 24 hours. Nitrous oxide (N_2O) concentration in the headspace gas samples was quantified using a gas chromatograph (Shimadzu GC-14A) equipped with an electron capture detector and a 6' x 1/8" SS Poropak Q 50/80 (Ohio Valley Specialty Chemical). Nitrous oxide production was converted from nmol N_2O to μmol N and areal denitrification rates were determined by dividing total N production by the original area of the sample.

Statistics

The effect of precipitation frequency on soil parameters and functions was examined using linear regression where appropriate and differences were considered significant at the $P < 0.05$ level. The linear regressions were performed using GraphPad Prism version 6.0b for Mac OS X. All of the relationships could be explained by a linear model with the exception of the first CO_2 flux measurement (Fig 5a). The correlation was non-linear and the variables contributing to that relationship remain unknown. Due to the lack of replicates, statistics could not be applied to the bacterial community data got from pyrosequencing.

Results

Bacterial community composition and diversity

Pyrosequencing analysis provided bacterial community composition and phylum-level trends for the precipitation gradient. Initial trimming and screening yielded a total of 44,375 sequences (average, 4,227 ± 1,925 sequences per treatment sample). Using a cut-

off at 97% similarity, a total of 2,188 OTUs was observed (average, 625 ± 85 OTUs per treatment sample). Bacterial community composition resolved at the phylum level is shown in Figure 2a. OTUs in all phyla were detected in all treatments with the exception of the candidate phyla OD1 and BRC1. OD1 was only represented in treatments 4 and 80 while BRC1 was represented in treatments 0, 8, 32, 60, 80, 100, and 120. The dominant phyla in every treatment were Cyanobacteria and Actinobacteria. Cyanobacterial sequences were more abundant than Actinomycetes in treatments 1, 2, 4, 8, 32, 100, and 120; the opposite was observed in the remaining treatments.

Proteobacteria, Bacteriodetes, Acidobacteria, and Chloroflexi were commonly represented in all treatments, followed by Planctomycetes and Gemmatimonadetes in lower relative abundance (Fig 2a). 13 of 14 common Proteobacteria phylotypes (>0.5% abundance) were Alphaproteobacteria (primarily orders Sphingomonadales and Rhizobiales) and the other was a Gammaproteobacterium (order Xanthomonadales). All common Bacteroidetes phylotypes were represented by the order Sphingobacteriales and the families Chitinophagaceae and Cytophagaceae. All common Acidobacteria were of subgroups Gp4 and Gp7. The most common non-cyanobacterial families by relative abundance were Geodermatophilaceae and Rubrobacteraceae (Actinobacteria), Gp4 (Actinobacteria), and Sphingomonadaceae (Proteobacteria).

Measured at a common sampling effort (2296 sequences per treatment), there was a significant negative correlation between OTU richness and precipitation frequency ($P = 0.0282$, $r^2 = 0.43$). The same was true for Shannon-Weaver Diversity Indices ($P = 0.0099$, $r^2 = 0.54$) (Fig 3a). The highest OTU richness and Shannon Diversity Index (710 and 8.5, respectively) was observed in treatment 8 and the lowest OTU richness and Shannon

Diversity Index (540 and 7.6, respectively) was observed in treatment 120, but because only one determination was available per treatment, the significance of this cannot be gauged.

Cyanobacterial community composition and diversity

Of the total 44,375 sequences, cyanobacterial accounted for about one quarter (10,449 total; 1,062 ± 667 cyanobacterial sequences per treatment). These could be assigned to a total of 151 OTUs (57 ± 16 OTUs per treatment), when defined with a 97% similarity cutoff. The relative abundances of the common (accounting for > 0.5 % of the total bacteria sequences) cyanobacterial OTUs are shown at each level of precipitation frequency in Figure 2b. Rare OTUs (<0.5% relative abundance) are shown as a composite group in the same figure. The common phylotypes are identified taxonomically based on a nearest identity (Blastn) analysis at the most discerning hierarchical level possible (i.e. *Microcoleus vaginatus* was assigned a single OTU but 7 different OTUs blasted nearest to a *M. steenstrupii* sequence in the database).

At a common sampling depth of 358 cyanobacterial sequences per treatment, we found significant negative correlations of both diversity ($P = 0.0119$, $r^2 = 0.52$) and OTU richness ($P = 0.0625$, $r^2 = 0.33$) to precipitation frequency (Fig 3b). OTU richness demonstrated only a weak tendency to decrease with increasing precipitation frequency. The highest cyanobacterial OTU richness and Shannon Diversity Index (73 and 5.0, respectively) was observed in treatment 2. The lowest cyanobacterial OTU richness (41) was observed in treatment 80 and the lowest Shannon Diversity Index (3.7) was observed in treatment 120. Again, significance cannot be tested and attributed here based on the lack of analytical replication.

Compositional community responses to frequency of precipitation (Bacterial)

Table 2 shows phylum abundance correlations with increasing precipitation frequency, as well as their corresponding statistical significance. Positive correlations were found for Acidobacteria and for the candidate phylum BRC1 ("bacterial rice cluster"). Planctomycetes and Proteobacteria showed negative trends. When only dominant OTUs were considered (>0.5% abundance), comparison between percent community composition and increasing precipitation showed positive correlations for Acidobacteria, Deinococcus-Thermus and negative correlation for Planctomycetes. Comparison between OTU richness and increasing precipitation at the phylum level showed positive correlation for BRC1 and negative for Planctomycetes. Weak negative correlations were also reported for Actinobacteria, OD1, and TM7. When only dominant OTUs were considered, comparison between OTU richness and precipitation frequency revealed a negative correlation for Cyanobacteria and positive linear correlations for Deinococcus-Thermus and Proteobacteria.

The number of dominant OTUs (>0.5 % abundance) was 109 out of 2179 total observed OTUs, or some 5%. Individual OTUs occurring in greater than 0.5% abundance of the total bacterial community and possessing significant correlations with increasing precipitation frequency (p values < 0.05) were extracted and reported in Table 3. Less than one-third (32 of 109) abundant bacterial phylotypes had significant correlations with precipitation.

Compositional community responses to frequency of precipitation (Cyanobacterial)

Common cyanobacterial OTUs (> 0.5% abundance of the total bacterial community) were evaluated for correlations with increasing precipitation frequency. The

26 common phylotypes are reported by their unique OTU identifier and assigned a name based on nearest identity Blastn to public databases in Table 4. Only 8 out of the 26 cyanobacterial phylotypes showed statistically significant correlations with precipitation frequency (Table 3). Nonetheless, other noteworthy patterns were observed for some phylotypes across the precipitation gradient. Most notably, OTU 2642 (*Leptolyngbya sp.*) was detected in every treatment but treatment 0 (lowest precipitation frequency) and OTU 2142 (*M. vaginatus*) occurred in the highest relative abundance of any OTU of any treatment in treatment 120 (11% of the total bacterial community, 40% of the total cyanobacterial community). Moreover, phylotypes 3980 (*M. steenstruppii*), 1522 (*Phormidium sp.*), 3726 (Oscillatoriales), and 2349 (*Leptolyngbya sp.*) were detected only in some treatments. Statistically significant, negative correlations with precipitation frequency were found for phylotypes 1337 (*M. steenstruppii*),1242 (*M. steenstruppii*), 1840 (*Microcoleus sp*.), 3993 (*Phormidium sp.*), and 3572 (*Leptolyngbya sp.*). We also found significant positive correlations for 3929 (*M. steenstruppii*), 1314 (*Microcoleus sp*.), and 2349 (*Leptolyngbya sp.*).

Soil pH and Chlorophyll a

Soil pH varied between 7.02 and 9.11 and positively correlated with increased precipitation frequency ($P<0.0001$, $r^2 = 0.72$; Fig 4a). The original untreated BSC (sampled from the field and measured in 2010) was measured to have a pH of 7.3 ± 0.15 (data not shown). Chlorophyll *a* concentrations in single determinations were between 1.2 mg chl *a* m^{-2} and 59 mg chl *a* m^{-2} and showed a weak tendency to increase with increasing precipitation frequency ($P = 0.0074$, $r^2 = 0.07$; Fig 4b).

Net, gross photosynthesis and dark respiration

In measurements made immediately after the treatment (see Materials and Methods), net areal photosynthetic rates appeared to positively correlate with precipitation frequency in a non-linear fashion but were not statistically confirmed. Net areal photosynthetic rates were entirely negative (CO_2 efflux) in treatments 0, 1, 2, and 8, crossing into the positive realm (no exchange or small CO_2 influx, respectively) in treatments 16, 32, and 60, and entirely positive (obvious CO_2 influx) in treatments 80, 100, and 120. Dark respiration rates measured after treatment appeared to correlate similarly with the strongest CO_2 efflux measured in treatments 0, 1, 2, 4, and 8 (not statistically confirmed).

CO_2 flux was measured a second time (15 days later) at which time we included diel cycle pre-conditioning under wet conditions. Net photosynthetic rates continued to positively correlate with precipitation frequency ($P < 0.0001$, $r^2 = 0.69$; Fig 5b), while dark respiration rates correlated more weakly ($P = 0.0001$, $r^2 = 0.39$). There was a pronounced recovery in the net photosynthetic rates for the low-performing treatments 0, 1, 2, 4 and 8, little or no change for treatments 32, 60, 80, 100 and 120, and an anomalous decrease in net photosynthetic rate for treatment 16. Net photosynthetic rates were entirely negative (CO_2 efflux) in treatments 1, 2, 4, 8, and 16, neutral or positive (no exchange or weak CO_2 influx) in treatments 0, 32, and 60, and entirely positive (clear CO_2 influx) in treatments 80, 100, and 120. Dark respiration rates also decreased markedly (reduced CO_2 efflux) with respect to initial measurements in treatments 0, 1, 2, 4, and 8 while somewhat increasing in treatments 80, 100, and 120.

Gross photosynthetic rates calculated as the difference from the previous measured parameters were similar for the initial and second CO_2 flux measurements and showed a weak positive correlation with increasing precipitation frequency (initial, $P = 0.0005$, $r^2 = 0.33$; second, $P = 0.0004$, $r^2 = 0.33$; Fig 5c).

Carbon substrate utilization

Carbon substrate utilization as determined by Biolog EcoPlates™ demonstrated ubiquitous diversity of carbon substrate metabolizing capability for all treatments and no correlation with precipitation frequency ($P = 0.19$, $r^2 = 0.06$) (Supplementary Data Fig. S2). At the end of the 168 h incubation, the EcoPlates™ incubated aerobically revealed an average community metabolic diversity (CMD) in all 11 treatments of 27 ± 2 carbon substrates utilized out of 31 tested. The EcoPlates™ incubated anaerobically were also observed after 168 h incubation and yielded an average CMD in all 11 treatments of 6 ± 3 carbon substrates utilized out of 31 tested, and no correlation to precipitation frequency ($P = 0.48$, $r^2 = 0.02$) (Fig. S3).

Nitrogen cycling

Analyses used for the determination of N_2-fixation potential, aerobic ammonia oxidation (AAO) potential, and denitrification potential revealed no trends across the precipitation gradient (Fig 9). Surprisingly there was no measurable N_2-fixation in any of the treatments, despite the fact that equivalent BSCs taken from the same sampling site had shown N_2-fixation in excess of 300 μmol N m^{-2} h^{-1} when measured soon after sampling in 2010 (data not shown). Rates of AAO potential were within those previously seen for desert BSCs (Strauss et al., 2012) but did not correlate with increasing or decreasing precipitation frequency ($P = 0.17$, $r^2 = 0.06$). No denitrification was detectable

outside of the margin of error, as similarly observed by (Johnson et al., 2007; Strauss et al., 2012).

Discussion

Community composition and diversity analysis

This study used high throughput pyrosequencing of PCR amplified 16s RNA genes to assess bacterial community composition and diversity. Perhaps expectedly, the number of OTUs observed (2,296) and the number of OTUs observed per sample (625 ± 85) was about 2 orders of magnitude larger that those previously reported in Sonoran desert BSCs (Nagy et al., 2005; Strauss et al., 2012) using molecular community fingerprinting techniques, like denaturing gradient gel electrophoresis (DGGE), that tend to emphasize common taxa and often fail to detect rare phylotypes. The average number of OTUs observed for each sample in this study (625 ± 85) is comparable, however, to a more recent pyrosequencing analysis of 10 varied Australian BSCs that yielded a range of 64-1018 total OTUs per sample (Abed et al., 2012). Interestingly, only 5% of those phylotypes gather more than 0.5% of all sequences (Table 2). Thus most of the phylotypes detected are quite rare and their relevance for major functional traits is questionable (Elshahed et al., 2008; Kunin et al., 2010; Shade et al., 2012). It must also be stated that the mere detection of 16s rDNA in the soil sample does not automatically indicate the viability of a given population since extracellular DNA can perpetuate for long periods of time in soils (Romanowski et al., 1992; Levy-Booth et al., 2007). The most precise conclusion that can be made is that, if detected, the population was present in the BSC at some time and its genomic DNA was not degraded prior to nucleic acid

extraction. Although still higher in richness, the treated BSC communities of this study represented by their abundant (common) phylotypes are in much better agreement with Sonoran desert BSC bacterial community composition observed by Nagy et al. (2005) and Strauss et al. (2012) who found 74 bacterial (19 cyanobacterial) common phylotypes and 30-33 bacterial (9-10 cyanobacterial), respectively.

We found general trends of decline in bacterial and cyanobacteria alpha diversity with increased frequency of precipitation, rather than the initially predicted maxima around frequencies typical of the Sonoran climate. In fact a maximum in OTU richness and diversity was observed in treatment 8, although this cannot be statistically resolved due to a lack of analytical replication in the pyrosequencing analysis. This treatment represents a relatively low precipitation frequency for the Sonoran desert (typically 20-30 pulses/year) with a mid-range drought length of 46 days (100-day droughts often occur between winter and summer monsoon precipitation). While BSC microorganisms are highly adapted to sustaining months-long periods of drought (Belnap, 2003c), the 46-day drought may indicate a threshold of maximal phylotype survival (given by minimal cellular/genomic degradation). As a consequence, lower OTU richness and diversity in treatments 0 to 4 may be explained by the loss of bacterial populations that did not withstand desiccation in excess of 46 days, in line with our second prediction. On the other hand, decreasing OTU richness and diversity with increased precipitation frequency can be attributed to increased competition between bacterial populations as drought stress diminished. OTU richness is mostly conserved across treatments 16 to 120 but then diversity drops off sharply in treatment 120, indicating that evenness was perturbed and a small number of populations were represented in higher relative abundance.

Alpha diversity metrics used to evaluate cyanobacterial richness and diversity showed similar patterns to those of all bacteria (Fig 3b). Interestingly, the maximal cyanobacterial OTU richness and diversity was at even lower precipitation frequency (treatment 2, 182-day drought interval), although this cannot be supported statistically as a real peak. If the apparent maximum and shift were real, it would suggest that the cyanobacterial community, on the whole, was more resilient to longer drought intervals than the general bacterial community. Regardless of the ability of the heterotrophic community to sustain and re-animate following a long drought, these data affirm the robust nature of the cyanobacterial phylotypes (to at least be detected) following a period of drought (182 days) that is rarely, if ever, experienced in the Sonoran desert. Lower diversity at high precipitation frequency perhaps reflects increased competition among the cyanobacterial phylotypes as the abiotic stress (water availability) was attenuated with increasing precipitation frequency, as previously described (Maestre et al., 2009). While the trends in composition are only relative, the fact that, on average, the Chl *a* concentrations (a proxy for cyanobacterial biomass) in the crusts only varied minimally, probably implies that the changes in relative abundance also reflect overall changes in population size, at least for this group of bacteria.

Cyanobacterial community composition and diversity

There were noticeable changes among the dominant cyanobacterial phylotypes comprising the cyanobacterial community (Fig 2b). It is important to state that a change in the relative abundance of one phylotype in different treatments only indicates a decrease or increase in the occurrence of the 16s rRNA genes for that phylotype; we cannot conclude that a change in relative abundance actually represents an increase or

decrease in the biomass of a particular phylotype. The clearest findings perhaps, were those of taxa becoming extinct in some treatments—of which there were several among the common cyanobacterial phylotypes. Upon close inspection, the common phylotypes seem to undergo a significant replacement from one end of the precipitation gradient to the other. Phylotypes that were only represented in the lower precipitation frequency treatments were likely more robust in maintaining cellular integrity over long intervals of drought and/or were simply outcompeted by less resilient but faster growing cyanobacterial phylotypes in treatments with more frequent precipitation. Conversely, phylotypes that were only found in treatments receiving high precipitation frequencies were likely unable to endure longer drought intervals and/or their fitness in higher precipitation frequency regimes provided an advantage over other cyanobacterial phylotypes . OTU 2142 (*M. vaginatus*) was the most, or second most, dominant single cyanobacterial OTU in all treatments with the exception of treatment 0, where it may have found its limit of drought tolerance. In treatment 120, however, OTU 2142 (*M. vaginatus*) greatly dominated all other phylotypes, suggesting that it was more competitive under that frequent precipitation regime.

The trends of the dominant cyanobacterial phylotypes that correlate with precipitation frequency are compelling within the context of previous BSC studies in deserts of the southwestern United States. *M. steenstrupii* and *M. vaginatus* have previously been shown to dominate BSCs of the Sonoran desert (Nagy et al., 2005), but it has recently been demonstrated by Garcia-Pichel et al. (in review) that *M. vaginatus* often dominates BSCs of cooler climates (higher latitudes and elevation), such as the Colorado Plateau, due to their increased psychrophylly (personal communication). The molecular

identification of *M. steenstrupii* and *M. vaginatus* is also confounded by the fact that the former has significantly greater genetic diversity than the latter (Boyer et al., 2002). While there was only a single phylotype observed for *M. vaginatus* in this analysis (100% identity), there were numerous phylotypes detected for *M. steenstrupii,* ranging from 96-99% identity. Moreover, it is possible that some phylotypes that assigned at lower taxonomic resolution (*Microcoleus sp*., *Phormidium sp*., and Oscillatoriales for example) may actually represent related *M. steenstrupii* phylotypes. Collectively, the *M. steenstrupii* phylotypes and potentially related phylotypes decreased in relative abundance with increasing precipitation frequency and were most prominently displaced by 2142 (*M. vaginatus*) and the *Leptolyngbya sp*. group in treatment 120. One explanation for this is that *M. vaginatus* continued to accumulate biomass through the cooler winter months of the treatment while most *M. steenstrupii* phylotypes were growth-restricted. Upon warming the following spring, *M. steenstrupii* phylotypes might not have been able to re-establish due to space, nutrient, and/or water limitations.

Shifts in the cyanobacterial community may have also been influenced by the nature of the treatment setup. The greenhouse installation inherently reduced the severity of some climate extremes experienced by the BSCs in their native condition. While air temperatures were equivalent, the treated BSCs did not experience the same surface temperatures and radiation exposure as those *in situ* (Belnap, 2003c) due to the filtering of some infrared and most ultraviolet radiation in the greenhouse setting. The attenuation of either of these natural stresses may have allowed for the propagation of phylotypes that would have otherwise experienced limitations or entirely succumbed in the native condition. In a similarly unnatural state, the effects of evaporative cooling repeatedly

afforded treatment 120 with every precipitation event could have additionally reduced the internal temperature of the BSC and resulted in the promotion of *M. vaginatus* growth, reducing the influence of summer temperature extremes. Furthermore, the establishment of *Leptolyngbya* phylotypes has not been observed previously in Sonoran desert BSCs (Nagy et al., 2005), although they have been observed in greater numbers and relative abundance in Mojave desert BSCs (Alwathnani and Johansen, 2011). Some regions of the Mojave Desert have lower mean annual temperatures and receive higher annual precipitation than the Sonoran desert (Rosentreter and Belnap, 2003) and it is possible that the *Leptolyngbya* phylotypes observed here were able to establish and thrive in higher precipitation frequency treatments in accordance with the conditions discussed above.

Phylum and phylotype responses to precipitation frequency

Among the common phylotypes 32 out of 109 OTUs showed significant trends with precipitation frequency. This speaks to the importance of this parameter in shaping community composition in BSCs. Some phylotypes responded positively and some negatively to precipitation, and their responses were only sometimes consistent within members of a single phylum. All 3 phylotypes of the Acidobacteria maintained positive correlations, for example, but phylotypes within the Actinobacteria, Bacteroidetes, Cyanobacteria, and Proteobacteria showed either positive or negative correlations. In these cases, of course any response patterns detected at the phylum level are the result of a few common phylotypes abounding, rather than a consistent trait generalizable to many members in the phylum. This exemplifies one of the problems with low-taxonomic-resolution community surveys: phyla are generally too diverse to infer functional

attributes. Many recent studies have also looked at correlations between bacterial groups and stress gradients, often demonstrating significant relationships at the phylum, class, or sub-class hierarchical levels (Lauber et al., 2009; Fierer et al., 2011; Eilers et al., 2012). Our data suggests that trends observed at those levels may not always be reliable, especially with regard to a BSC.

A note of caution

The significant increase in pH with increasing precipitation frequency was not anticipated and complicates the interpretation of the trends observed in this study. Treatments 0 to 16 were mostly consistent with the pH originally measured *in situ* (7.3 ± 0.15) and the most pronounced pH increases were observed in the treatments receiving the highest precipitation frequency, 32 to 120 (Fig 4a). It is clear that precipitation frequency influenced the pH but we do not know if this was a direct or indirect effect. It is possible that an increase in alkalinity was derived from increased evaporation of dissolved CO_2. Regardless of the cause of the pH increase seen, in a rigorous way, is not possible to determine whether the biotic changes across the precipitation gradient were also influenced by the pH shift or otherwise contributed to it. Many studies have demonstrated that soil pH is one of the strongest drivers of soil bacterial community diversity (Fierer and Jackson, 2006; Lauber et al., 2009; Fierer et al., 2011). Generally, soil bacterial diversity tends to peak near neutral pH and then suffers declines with increasing acidity or alkalinity. Soils with pH values above neutral have been studied to a lesser extent, although data from the aforementioned studies indicates a general trend of declining soil bacterial diversity with increasing alkalinity (only studied in soils up to pH 9).

Net photosynthesis, gross photosynthesis and dark respiration

CO_2 exchange rates were measured twice for every treated sample and revealed a great deal about the influences of precipitation frequency on BSC carbon dynamics. The initial measurement was considered to be an activation of the community in order to measure the true physiological potential after a given interval of preceding drought. Here we found clear trends with frequency of precipitation for both dark respiration and net photosynthesis. In the first measurement, treatments 0 to 8 exhibited substantial carbon efflux in both light (net photosynthesis) and dark (dark respiration) (Fig 5a). This result is in agreement with previous studies that demonstrated the propensity of BSC to trend toward exhaustive respiration following extended periods of drought and/or small precipitation pulses (Belnap et al., 2004; Johnson et al., 2012). It is postulated that, if continued, this response can give rise to a C deficit that will result in the loss of BSC biomass, even entire BSC cover, as C is respired away. However, the gross photosynthesis calculated for treatments 0 to 8 in this first measurement (Fig 5c), shows that photosynthesis occurred at similar rates through the gradient of treatments (except treatment 100). This implies that the effects seen in net photosynthesis were fully driven by the enhancement of respiration with intense drought. This is consistent with the fact that cyanobacterial biomass (as Chl *a*) only varied minimally with increased precipitation, again except for treatment 100, where it was considerably higher. Belnap et al. 2004 and Johnson et al. 2012 argued that the C deficit was partly due to negative effects of drought on photosynthesis, but we can show here that it must be squarely attributed to a robust respiring heterotrophic community. This respiratory pulse can be explained by osmotic shock upon rewetting and the subsequent lysis of microbial cells

and/or the release of intracellular solutes, providing substrate to be mineralized by the viable microbial community (Fierer and Schimel, 2002).

In our second set of CO_2 exchange rates, where we allowed for a 24 h period of physiological recovery, there was pronounced reduction in the degree of C efflux in treatments 0 to 8 (Fig 5b), indicating that the enhancement of respiration by drought is transient, potentially as a result of an eventual reduction in the pool of C substrate available for mineralization. The majority of treatments also demonstrated greater gross photosynthesis in the second round of measurements (Fig 5c), with a notable increase in the degree of C efflux in treatments 80 to 120. This may be due to the availability of photosynthate accumulated during the first and second light measurements and the pre-conditioning period of the second measurement.

Carbon substrate utilization

There was no correlation between carbon substrate utilization potential and precipitation frequency, indicating that there was no loss of function with precipitation frequency alteration. Any of the relative changes in particular phylotypes detected, must have been insufficient to wipe out their potential for recovery in this long-term assay. Alternatively, compositional changes could have brought along high functional redundancy, so that changes in community were not reflected changes in functions.

Nitrogen cycling

The alteration of precipitation frequency did not significantly influence any nitrogen cycling process in the treated BSCs (Fig 6). However, the loss of N fixation across all treatments was a curious find. As previously mentioned, equivalent BSCs taken from the same sampling site had shown N fixation rates in excess of 300 μmol N m^{-2} h^{-1}.

It is possible that this was the result of our incubation setup being within an urban setting since urban atmospheric N deposition can be high (Vitousek et al., 1997; Fenn et al., 2003). The crusts were sampled in a rural setting at least 20 miles outside of a major city and transported for treatment in the infamously polluted atmosphere of the greater metropolitan area of Phoenix, Arizona. N-fixers may have shut down the energy-intensive fixation of N_2 as a result (Belnap and Eldridge, 2003). Additionally, the cyanolichen *Collema sp.*, originally observed on the BSC surface at the time of sampling, was ostensibly reduced in abundance by the end of the treatment, if not erased altogether in some treatments. Lichens have long been identified as very sensitive pollution indicators (Conti and Cecchetti, 2001), therefore, N fixation in the treated BSCs may have been primarily impacted by the loss of *Collema sp.* lichen due to toxifying pollution. This is supported by the fact that the cyanobiont of *Collema sp.*, *Nostoc sp*., was not detected in the pyrosequencing analysis, whereas other free-living crust N_2-fixers (Yeager et al., 2007)were present and detected (*Tolypothrix sp*. and *Scytonema sp*).

Aerobic ammonia oxidation (AAO) potential was detected in all treated samples but revealed no correlation with precipitation frequency. The magnitude of AAO was within ranges previously described for desert BSCs (Strauss et al., 2012). Interestingly, the function of ammonia oxidation was maintained even when N fixation was not detected. This suggests that the ammonia oxidizers are robust with regard to desiccation tolerance and persist until ammonia is available again and/or utilize sources of ammonia produced by ammonification (Miralles et al., 2012). Denitrification was not detected in any treatments, in agreement with previous BSC studies (Johnson et al., 2007; Strauss et al., 2012). If desiccation tolerance were limiting to the presence of denitrifiers, we

anticipated that increased precipitation frequency could allow for the establishment of denitrifying populations but this was not observed.

Conclusions

We conclude that the Sonoran desert BSC studied here was primarily resistant to the influence of altered precipitation frequency with regard to bacterial community structure and function as demonstrated by complementing molecular and functional analysis. While bacterial community diversity was subject to perturbation with increasing precipitation frequency, the collective functions analyzed showed no real negative impacts as a result of taxonomic diversity loss. This suggests that either 1) there were no functional losses with precipitation frequency alteration or 2) the BSC microbial community originally possessed a sufficiently high functional redundancy that effectively obscured any functional losses caused by this treatment.

REFERENCES

Abed, R.M.M., Ramette, A., Hübner, V., Deckker, P., Beer, D., 2012. Microbial diversity of eolian dust sources from saline lake sediments and biological soil crusts in arid Southern Australia. FEMS Microbiology Ecology 80, 294–304.

Acosta-Martínez, V., Dowd, S., Sun, Y., Allen, V., 2008. Tag-encoded pyrosequencing analysis of bacterial diversity in a single soil type as affected by management and land use. Soil Biology and Biochemistry 40, 2762–2770.

Alwathnani, H., Johansen, J.R., 2011. Cyanobacteria in soils from a Mojave Desert ecosystem. Monographs of the Western North American Naturalist 5, 71–89.

Bachar, A., Al-Ashhab, A., Soares, M.I.M., Sklarz, M.Y., Angel, R., Ungar, E.D., Gillor, O., 2010. Soil microbial abundance and diversity along a low precipitation gradient. Microbial Ecology 60, 453–461.

Bates, S.T., Garcia-Pichel, F., 2009. A culture-independent study of free-living fungi in biological soil crusts of the Colorado Plateau: their diversity and relative contribution to microbial biomass. Environmental Microbiology 11, 56–67.

Belnap, J., 2002. Nitrogen Fixation in Biological Soil Crusts From Southeast Utah, USA. BIOLOGY AND FERTILITY OF SOILS 35, 128–135.

Belnap, J., 2003a. Influence of biological soil crusts on soil environments and vasuclar plants, in: Belnap, J., Lange, O.L. (Eds.), Biological Soil Crusts: Structure, Function, and Management. Springer-Verlap, Berlin, pp. 281–300.

Belnap, J., 2003b. Biological soil crusts and wind erosion, in: Belnap, J., Lange, O.L. (Eds.), Biological Soil Crusts: Structure, Function, and Management. Springer-Verlap, Berlin, pp. 339–347.

Belnap, J., 2003c. Biological soil crusts: characteristics and distribution, in: Belnap, J., Lange, O.L. (Eds.), Biological Soil Crusts: Structure, Function, and Management. Springer-Verlap, Berlin, pp. 3–30.

Belnap, J., Eldridge, D.J., 2003. Disturbance and recovery of biological soil crusts., in: Belnap, J., Lange, O.L. (Eds.), Biological Soil Crusts: Structure, Function, and Management. Springer-Verlap, Berlin, pp. 363–383.

Belnap, J., Phillips, S., Miller, M., 2004. Response of desert biological soil crusts to alterations in precipitation frequency. Oecologia 141, 306–316.

Bowker, M.A., Maestre, F.T., Escolar, C., 2010. Biological crusts as a model system for examining the biodiversity-ecosystem function relationship in soils. Soil Biology and Biochemistry 42, 405–417.

Boyer, S.L., Johansen, J.R., Flechtner, V.R., Howard, G.L., 2002. Phylogeny and genetic variance in terrestrial *Microcoleus* (Cyanophyceae) species based on sequence analysis of the 16S rRNA gene and associated 16S–23S ITS region. Journal of Phycology 38, 1222–1235.

Büdel, B., Darienko, T., Deutschewitz, K., Dojani, S., Friedl, T., Mohr, K.I., Salisch, M., Reisser, W., Weber, B., 2008. Southern African biological soil crusts are ubiquitous and highly diverse in drylands, being restricted by rainfall frequency. Microbial Ecology 57, 229–247.

Caporaso, J.G., Bittinger, K., Bushman, F.D., DeSantis, T.Z., Andersen, G.L., Knight, R., 2010. PyNAST: a flexible tool for aligning sequences to a template alignment. Bioinformatics 26, 266–267.

Caporaso, J.G., Kuczynski, J., Stombaugh, J., Bittinger, K., Bushman, F.D., Costello, E.K., Fierer, N., Peña, A.G., Goodrich, J.K., Gordon, J.I., Huttley, G.A., Kelley, S.T., Knights, D., Koenig, J.E., Ley, R.E., Lozupone, C.A., McDonald, D., Muegge, B.D., Pirrung, M., Reeder, J., Sevinsky, J.R., Turnbaugh, P.J., Walters, W.A., Widmann, J., Yatsunenko, T., Zaneveld, J., Knight, R., 2010. QIIME allows analysis of high-throughput community sequencing data. Nature Methods 7, 335–336.

Christensen, J.H., 2007. IPCC Chapter 11 Regional 1–94.

Conti, M.E., Cecchetti, G., 2001. Biological monitoring: lichens as bioindicators of air pollution assessment—a review. Environmental Pollution 114, 471–492.

Cook, E.R., Seager, R., Heim, R.R., Jr, Vose, R.S., Herweijer, C., Woodhouse, C., 2010. Megadroughts in North America: placing IPCC projections of hydroclimatic change in a long-term palaeoclimate context. Journal of Quaternary Science 25, 48–61.

DeSantis, T.Z., Hugenholtz, P., Larsen, N., Rojas, M., Brodie, E.L., Keller, K., Huber, T., Dalevi, D., Hu, P., Andersen, G.L., 2006. Greengenes, a chimera-checked 16S rRNA gene database and workbench compatible with ARB. Applied and Environmental Microbiology 72, 5069–5072.

Edgar, R.C., 2010. Search and clustering orders of magnitude faster than BLAST. Bioinformatics 26, 2460–2461.

Eilers, K.G., Debenport, S., Anderson, S., Fierer, N., 2012. Digging deeper to find unique microbial communities: The strong effect of depth on the structure of bacterial and archaeal communities in soil. Soil Biology and Biochemistry 50, 58–65.

Elshahed, M.S., Youssef, N.H., Spain, A.M., Sheik, C., Najar, F.Z., Sukharnikov, L.O., Roe, B.A., Davis, J.P., Schloss, P.D., Bailey, V.L., Krumholz, L.R., 2008. Novelty and uniqueness patterns of rare members of the soil biosphere. Applied and Environmental Microbiology 74, 5422–5428.

Evans, R.D., Lange, O.L., 2003. Biological soil crusts and ecosystem nitrogen and carbon dynamics, in: Belnap, J., Lange, O.L. (Eds.), Biological Soil Crusts: Structure, Function, and Management. Springer-Verlap, Berlin, pp. 263–279.

Fenn, M.E., Baron, J.S., Allen, E.B., Rueth, H.M., Nydick, K.R., Geiser, L., Bowman, W.D., Sickman, J.O., Meixner, T., Johnson, D.W., 2003. Ecological effects of nitrogen deposition in the western United States. BioScience 53, 404–420.

Fierer, N., Jackson, R.B., 2006. The diversity and biogeography of soil bacterial communities. Proceedings of the National Academy of Sciences of the United States of America 103, 626–631.

Fierer, N., McCain, C.M., Meir, P., Zimmermann, M., Rapp, J.M., Silman, M.R., Knight, R., 2011. Microbes do not follow the elevational diversity patterns of plants and animals. Ecology Letters 92, 797–804.

Fierer, N., Schimel, J.P., 2002. Effects of drying-rewetting frequency on soil carbon and nitrogen transformations. Soil Biology and Biochemistry 34, 777–787.

Garcia-Pichel, F., Belnap, J., 1996. Microenvironments and microscale productivity of cyanobacterial desert crusts. Journal of Phycology 32, 774–782.

Garcia-Pichel, F., López-Cortés, A., Nübel, U., 2001. Phylogenetic and morphological diversity of cyanobacteria in soil desert crusts from the Colorado plateau. Applied and Environmental Microbiology 67, 1902–1910.

Gilbert, J.A., Steele, J.A., Caporaso, J.G., Steinbrück, L., Reeder, J., Temperton, B., Huse, S., McHardy, A.C., Knight, R., Joint, I., Somerfield, P., Fuhrman, J.A., Field, D., 2012. Defining seasonal marine microbial community dynamics. The ISME Journal 6, 298–308.

Groffman, P.M., Tiedje, J., 1989. Denitrification in north temperate forest soils—spatial and temporal patterns at the landscape and seasonal scales. Soil Biology and Biochemistry 21, 613–620.

Gundlapally, S.R., Garcia-Pichel, F., 2006. The community and phylogenetic diversity of biological soil crusts in the Colorado Plateau studied by molecular fingerprinting and intensive cultivation. Microbial Ecology 52, 345–357.

Haas, B.J., Gevers, D., Earl, A.M., Feldgarden, M., Ward, D.V., Giannoukos, G., Ciulla, D., Tabbaa, D., Highlander, S.K., Sodergren, E., Methe, B., DeSantis, T.Z., The Human Microbiome Consortium, Petrosino, J.F., Knight, R., Birren, B.W., 2011. Chimeric 16S rRNA sequence formation and detection in Sanger and 454-pyrosequenced PCR amplicons. Genome Research 21, 494–504.

Jeffries, D.L., Klopatek, J.M., Link, S.O., Bolton, H., Jr, 1992. Acetylene reduction by cryptogamic crusts from a blackbrush community as related to resaturation and dehydration. Soil Biology and Biochemistry 24, 1101–1105.

Johnson, S.L., Budinoff, C.R., Belnap, J., Garcia-Pichel, F., 2005. Relevance of ammonium oxidation within biological soil crust communities. Environmental Microbiology 7, 1–12.

Johnson, S.L., Kuske, C.R., Carney, T.D., Housman, D.C., Gallegos-Graves, L.V., Belnap, J., 2012. Increased temperature and altered summer precipitation have differential effects on biological soil crusts in a dryland ecosystem. Global Change Biology 18, 2583–2593.

Johnson, S.L., Neuer, S., Garcia-Pichel, F., 2007. Export of nitrogenous compounds due to incomplete cycling within biological soil crusts of arid lands. Environmental Microbiology 9, 680–689.

Kunin, V., Engelbrektson, A., Ochman, H., Hugenholtz, P., 2010. Wrinkles in the rare biosphere: pyrosequencing errors can lead to artificial inflation of diversity estimates. Environmental Microbiology 12, 118–123.

Lauber, C.L., Hamady, M., Knight, R., Fierer, N., 2009. Pyrosequencing-based assessment of soil pH as a predictor of soil bacterial community structure at the continental scale. Applied and Environmental Microbiology 75, 5111–5120.

Levy-Booth, D.J., Campbell, R.G., Gulden, R.H., Hart, M.M., Powell, J.R., Klironomos, J.N., Pauls, K.P., Swanton, C.J., Trevors, J.T., Dunfield, K.E., 2007. Cycling of extracellular DNA in the soil environment. Soil Biology and Biochemistry 39, 2977–2991.

Maestre, F.T., Martinez, I., Escolar, C., Escudero, A., 2009. On the relationship between abiotic stress and co-occurrence patterns: an assessment at the community level using soil lichen communities and multiple stress gradients. Oikos 118, 1015–1022.

Miralles, I., Domingo, F., García-Campos, E., Trasar-Cepeda, C., Leirós, M.C., Gil-Sotres, F., 2012. Biological and microbial activity in biological soil crusts from the Tabernas desert, a sub-arid zone in SE Spain. Soil Biology and Biochemistry 55, 113–121.

Nagy, M.L., PÃ rez, A., Garcia-Pichel, F., 2005. The prokaryotic diversity of biological soil crusts in the Sonoran Desert (Organ Pipe Cactus National Monument, AZ). FEMS Microbiology Ecology 54, 233–245.

Overpeck, J., Udall, B., 2010. Dry times ahead. Science 328, 1642–1643.

Potts, M., 1994. Desiccation tolerance of prokaryotes. Microbiological reviews 58, 755–805.

Price, M.N., Dehal, P.S., Arkin, A.P., 2010. FastTree 2--approximately maximum-likelihood trees for large alignments. PLoS ONE 5, e9490.

Rivera-Aguilar, V., GodInez-Alvarez, H., Moreno-Torres, R., RodrIguez-Zaragoza, S., 2009. Soil physico-chemical properties affecting the distribution of biological soil crusts along an environmental transect at Zapotitlan drylands, Mexico. Journal of Arid Environments 73, 1023–1028.

Romanowski, G., Lorenz, M.G., Sayler, G., Wackernagel, W., 1992. Persistence of free plasmid DNA in soil monitored by various methods, including a transformation assay. Applied and Environmental Microbiology 58, 3012–3019.

Rosentreter, R., Belnap, J., 2003. Biological soil crusts of North America, in: Belnap, J., Lange, O.L. (Eds.), Biological Soil Crusts: Structure, Function, and Management. Springer-Verlap, Berlin, pp. 31–50.

Seager, R., Ting, M., Held, I., Kushnir, Y., Lu, J., Vecchi, G., Huang, H.P., Harnik, N., Leetmaa, A., Lau, N.C., Li, C., Velez, J., Naik, N., 2007. Model projections of an imminent transition to a more arid climate in southwestern North America. Science 316, 1181–1184.

Shade, A., Hogan, C.S., Klimowicz, A.K., Linske, M., McManus, P.S., Handelsman, J., 2012. Culturing captures members of the soil rare biosphere. Environmental Microbiology 14, 2247–2252.

Strauss, S.L., Day, T.A., Garcia-Pichel, F., 2012. Nitrogen cycling in desert biological soil crusts across biogeographic regions in the Southwestern United States. Biogeochemistry 108, 171–182.

Vitousek, P.M., Aber, J.D., Howarth, R.W., Likens, G.E., Matson, P.A., Schindler, D.W., Schlesinger, W.H., Tilman, D.G., 1997. Human alteration of the global nitrogen cycle: sources and consequences. Ecological Applications 7, 737–750.

Wang, Q., Garrity, G.M., Tiedje, J.M., Cole, J.R., 2007. Naive Bayesian classifier for rapid assignment of rRNA sequences into the new bacterial taxonomy. Applied and Environmental Microbiology 73, 5261–5267.

Warren, S.D., 2003. Biological soil crusts and hydrology in North American deserts, in: Belnap, J., Lange, O.L. (Eds.), Biological Soil Crusts: Structure, Function, and Management. Springer-Verlap, Berlin, pp. 327–337.

Weiss, J.L., Overpeck, J.T., 2005. Is the Sonoran Desert losing its cool? Global Change Biology 11, 2065–2077.

Yeager, C.M., Kornosky, J.L., Morgan, R.E., Cain, E.C., Garcia-Pichel, F., Housman, D.C., Belnap, J., Kuske, C.R., 2007. Three distinct clades of cultured heterocystous cyanobacteria constitute the dominant N_2-fixing members of biological soil crusts of the Colorado Plateau, USA. FEMS Microbiology Ecology 60, 85–97.

Table 1 Types of sampling strategies used in the structural and functional characterization of soil crusts

Strategy	Sampling Impact	Method	Specifications	Purposed Analysis/Analyses
A	Non-Destructive	collar insertion	1 circular impression, 9 cm diameter and 1.5 mm wide	• CO_2 flux
B	Destructive	BSC cores removed	Soil corer (11 mm diameter; 95 mm^2) inserted to a depth of 1 cm, 3 replicates per sample, 9 replicates per treatment. Moist cores were air-dried at 25°C for 36 hours and then homogenized with a sterile spatula. The resulting homogenate was sandy with no intact BSC remaining. The samples were stored at -80°C until processing.	• pH • Nucleic acid extraction
C	Destructive	BSC cores removed	Soil corer (11 mm diameter; 95 mm2) inserted to a depth of 1 cm, 3 replicates per sample, 9 replicates per treatment.	• Chl *a* extraction
D	Destructive	BSC removed	Sampled for a known surface area to 1 cm depth. Mass to volume ratio was approximately 1 g for 1 cm^3. Samples were transferred to a sterile petri dish and homogenized with a sterile spatula. The resulting homogenate was sandy with no intact BSC remaining.	• Potential Aerobic Ammonia Oxidation • Potential Denitrification • Carbon substrate utilization diversity • Sulfate reduction potential
E	Destructive	BSC removed	Sampled for a known surface area to 1 cm depth, BSC structure intact. Mass to volume ratio was approximately 1 g for 1 cm^3	• Potential Nitrogen fixation

Table 2 Correlation with precipitation frequency of the relative representation of different bacterial phyla

	All Phylotypes Observed					Phylotypes of >.5% Abundance				
	OTUs	% Community Composition Precipitation Correlation		OTU Richness Precipitation Correlation		OTUs	% Community Composition Precipitation Correlation		OTU Richness Precipitation Correlation	
			R^2, p value		R^2, p value			R^2, p value		R^2, p value
Acidobacteria	123	+	**0.720 (0.001)**			7	+	**0.796 (<0.001)**		
Actinobacteria	315			-	0.310 (0.075)	17				
Bacteroidetes	228					16				
BRC1	5	+	**0.679 (0.002)**	+	**0.563 (0.008)**	--				
Chloroflexi	149					6				
Cyanobacteria	151					26			-	**0.710 (0.001)**
Chloroplast	8					3				
Deinococcus-Thermus	8					1	+	**0.514 (0.013)**	+	**0.642 (0.003)**
Fermicutes	14					--				
Gemmatimonadetes	67					--				
Nitrospira	6					--				
ODI	1			-	0.304 (0.079)	--				
OPI0	3					1				
Planctomycetes	116	-	**0.758 (<0.001)**	-	**0.658 (0.003)**	1	-	**0.407 (0.035)**		
Proteobacteria	378	-	**0.405 (0.035)**			14			+	0.286 (0.090)
TM7	14			-	0.307 (0.077)	--				
Verrucomicrobia	31					--				
Unclassified	562					17	+	**0.432 (0.028)**	+	**0.501 (0.015)**
Total OTUs	2179					109				

Bold values indicate a significance of <0.05, remaining values are significant <0.1.
+ positive correlation of abundance with increasing precipitation frequency
- negative correlation of abundance with increasing precipitation frequency

Table 3 List of OTUs that show correlations with precipitation frequency (common phylotypes)

Phylum	RDP Taxonomy Assignment	% Community Composition Precipitation Correlation	R^2, p value
Acidobacteria	Acidobacteria_Gp4; Gp4	+	0.8093 (0.0002)
	Acidobacteria_Gp4; Gp4	+	0.6299 (0.0035)
	Acidobacteria_Gp7; Gp7	+	0.0333 (0.4118)
Actinobacteria	Actinobacteria	+	0.4748 (0.019)
	Solirubrobacterales; Solirubrobacteraceae; Solirubrobacter	-	0.4092 (0.0341)
Bacteroidetes	Sphingobacteria; Sphingobacteriales; Chitinophagaceae	-	0.7824 (0.0003)
	Sphingobacteria; Sphingobacteriales; Cytophagaceae; Hymenobacter	+	0.5993 (0.0052)
	Sphingobacteria; Sphingobacteriales; Chitinophagaceae	-	0.5833 (0.0063)
	Sphingobacteria; Sphingobacteriales; Chitinophagaceae; Flavisolibacter	+	0.4441 (0.0251)
	Sphingobacteriales; Cytophagaceae; Adhaeribacter	+	0.4387 (0.0264)
	Sphingobacteria; Sphingobacteriales	+	0.3941 (0.0387)
	Sphingobacteria; Sphingobacteriales	-	0.3905 (0.0398)
	Sphingobacteria; Sphingobacteriales; Chitinophagaceae	-	0.3834 (0.0422)
Chloroflexi	Chloroflexi	+	0.479 (0.0183)
	Chloroflexi	+	0.3715 (0.0465)
Cyanobacteria	Cyanobacteria (3993; *Phormidium sp.*)	-	0.7119 (0.0011)
	Family XIII; GpXIII (3929; *M. steenstrupii*)	+	0.6089 (0.0046)
	Cyanobacteria (1337; *M. steenstrupii*)	-	0.5545 (0.0086)
	Cyanobacteria (3572; *Letpolyngbya sp.*)	-	0.5087 (0.0137)
	Cyanobacteria (1840; *Microcoleus sp.*)	-	0.4361 (0.027)
	Cyanobacteria (2349; *Leptolyngbya sp.*)	+	0.4162 (0.0321)
	Cyanobacteria (1242; *M. steenstrupii*)	-	0.4026 (0.036)
	Family XIII; GpXIII (1314; *Microcoleus sp.*)	+	0.3744 (0.0454)
Deinococcus-Thermus	Deinococci; Deinococcales; Trueperaceae; Truepera	+	0.5135 (0.0131)
Planctomycetes	Planctomycetacia; Planctomycetales; Planctomycetaceae; Singulisphaera	-	0.407 (0.0347)
Proteobacteria	Alphaproteobacteria; Sphingomonadales; Sphingomonadaceae; Sphingomonas	+	0.7592 (0.0005)
	Alphaproteobacteria; Rhizobiales	-	0.5529 (0.0087)
	Alphaproteobacteria; Rhizobiales	-	0.4651 (0.0208)
	Alphaproteobacteria; Sphingomonadales; Sphingomonadaceae; Sphingomonas	+	0.4048 (0.0353)
	Alphaproteobacteria; Sphingomonadales; Erythrobacteraceae; Altererythrobacter	+	0.3874 (0.0408)
Unclassified Bacteria	Bacteria	+	0.8407 (<0.0001)
	Bacteria	+	0.5953 (0.0054)

+ positive correlation of abundance with increasing precipitation frequency

- negative correlation of abundance with increasing precipitation frequency

Cyanobacteria (OTU identifier; nearest blastn match)

Table 4 Common cyanobacterial phylotypes (>0.5% abundance) and their nearest BLASTn match in GenBank

Accession Number	OTU ID	Closest Relative	Similarity (%)
JQ712615.1	2142	*Microcoleus vaginatus*	100
AF355386.1	2733	*Microcoleus steenstrupii*	97
AF355386.1	1337	*Microcoleus steenstrupii*	96
AF355386.1	106	*Microcoleus steenstrupii*	97
AF355380.1	3929	*Microcoleus steenstrupii*	97
AF355392.1	1242	*Microcoleus steenstrupii*	99
AF355395.1	2634	*Microcoleus steenstrupii*	99
AF355386.1	3980	*Microcoleus steenstrupii*	99
CP003632.1	590	*Microcoleus sp.*	95
EU586738.1	1215	*Microcoleus sp.*	100
EF654075.1	1840	*Microcoleus sp.*	100
EU586738.1	1314	*Microcoleus sp.*	93
EU196618.1	3445	Phormidiaceae	98
EF654065.1	3993	*Phormidium sp.*	96
EF654065.1	434	*Phormidium sp.*	98
EU196618.1	1522	*Phormidium sp.*	96
FJ790622.1	3726	Oscillatoriales	96
HQ847553.1	1630	*Scytonema sp.*	99
EU586743.1	2032	*Leptolyngbya sp.*	99
EU586743.1	2642	*Leptolyngbya sp.*	97
AY239604.1	3572	*Leptolyngbya sp.*	100
DQ786166.1	2349	*Leptolyngbya sp.*	99
FJ805921.1	3087	*Chroococcidiopsis*	99
FJ805921.1	187	*Chroococcidiopsis*	93
AF334693.1	1071	*Tolypothrix sp.*	99
EF654073.1	2518	Pseudanabaenaceae	100

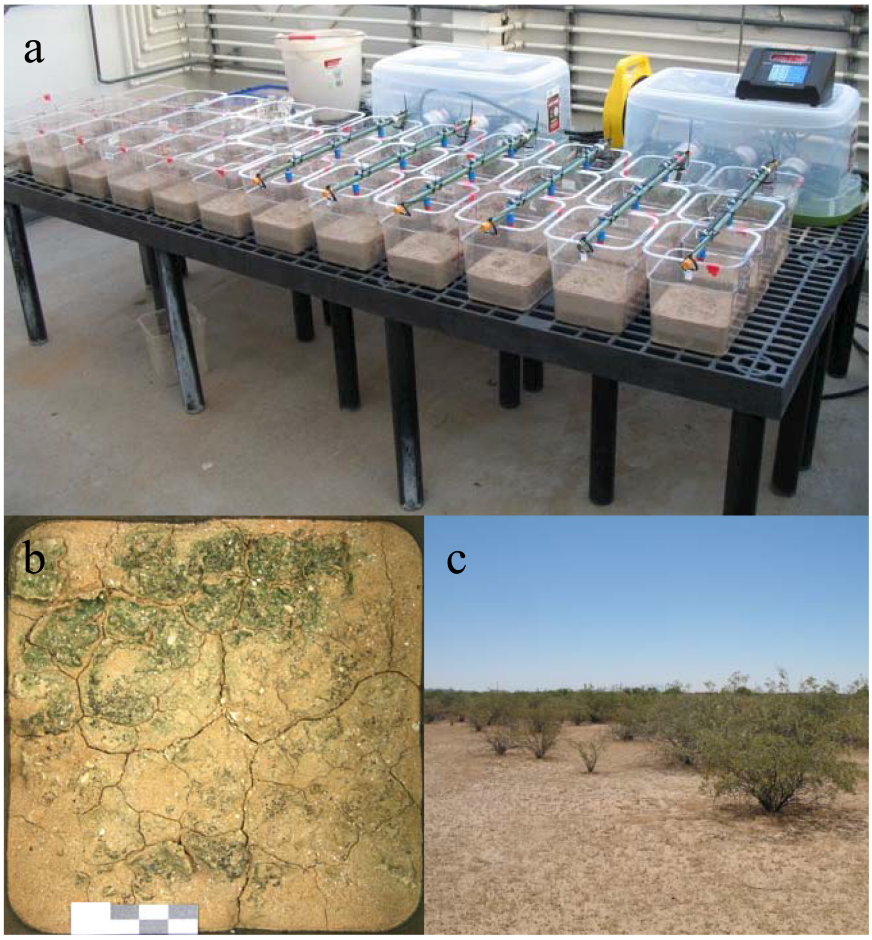

Figure 1 **BSC sampling site and microcosm setup. a)** Microcosm precipitation gradient treatment installation in greenhouse. **b)** Overhead view of BSC microcosm treated with 80 days/yr precipitation frequency at the end of the precipitation treatment (black bars = 1 cm). **c)** Field site, Casa Grande, AZ

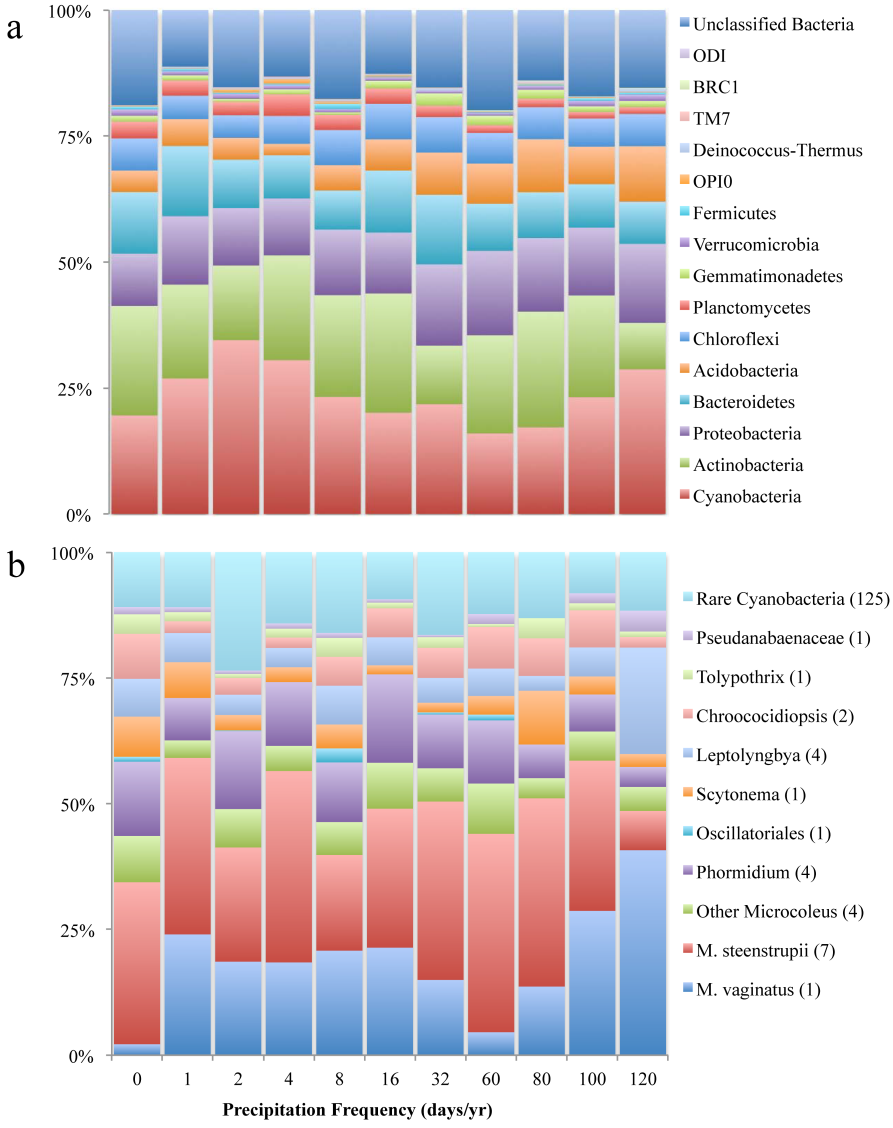

Figure 2 **Community structure determined by pyrosequencing analysis of 16S rRNA genes as a function of altered precipitation frequency treamtment. a)** Bacterial community structure, resolved at phylum level. **b)** Cyanobacterial community structure, resolved at generic level. Common cyanobacterial OTUs (greater than 0.5% representation) assigned the taxonomic epithet of the nearest identity Blastn analysis. 'Rare Cyanobacteria' are OTUs represented in less than 0.5% abundance and are grouped together. Number in parentheses indicates number of OTUs in that grouping.

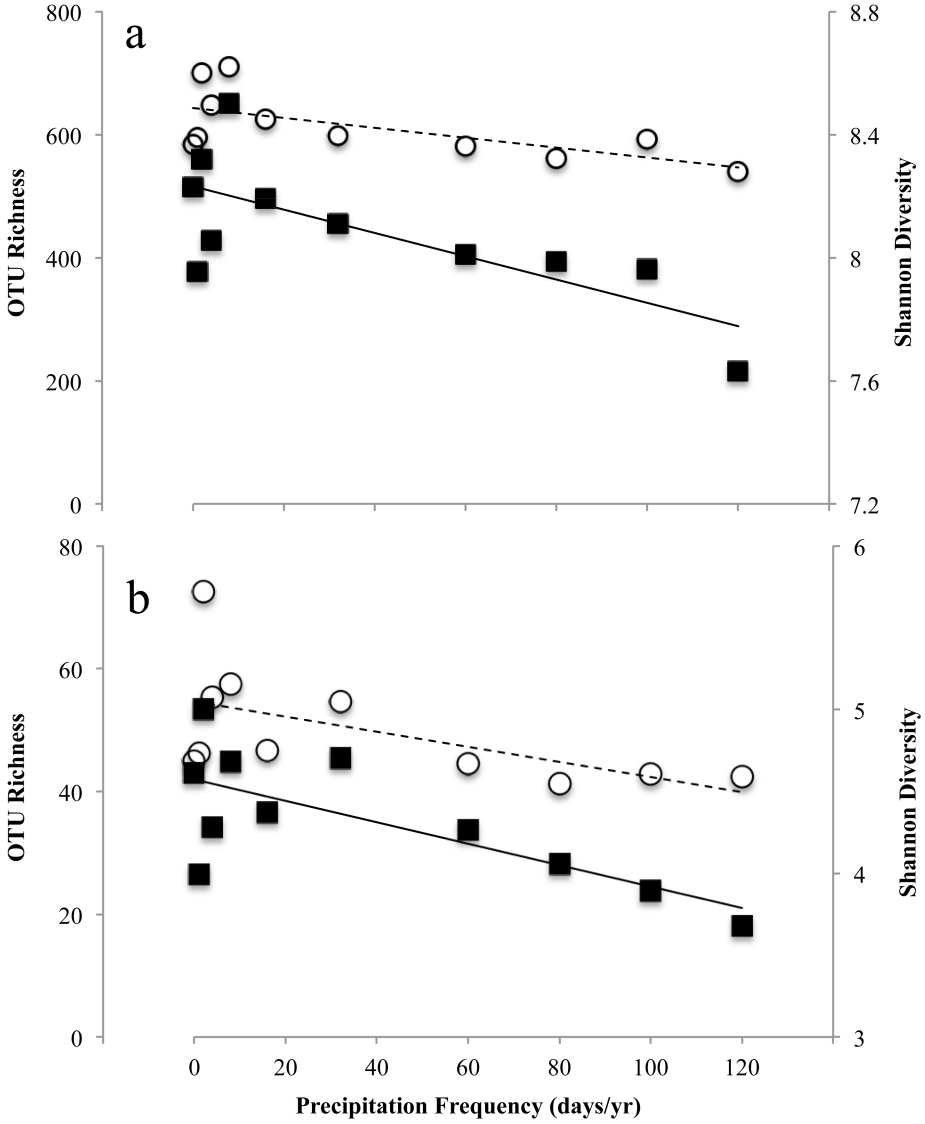

Figure 3 **Alpha diversity metrics based on molecular community composition as a function of altered precipitation frequency treatment. a)** Bacterial community; Shannon diversity index (■) and richness (○) determined at a sampling effort of 2296 sequences per treatment. **b)** Cyanobacterial community; Shannon diversity index (■) and OTU richness (○) determined at a sampling effort of 358 sequences per treatment. Lines are linear regressions for each.

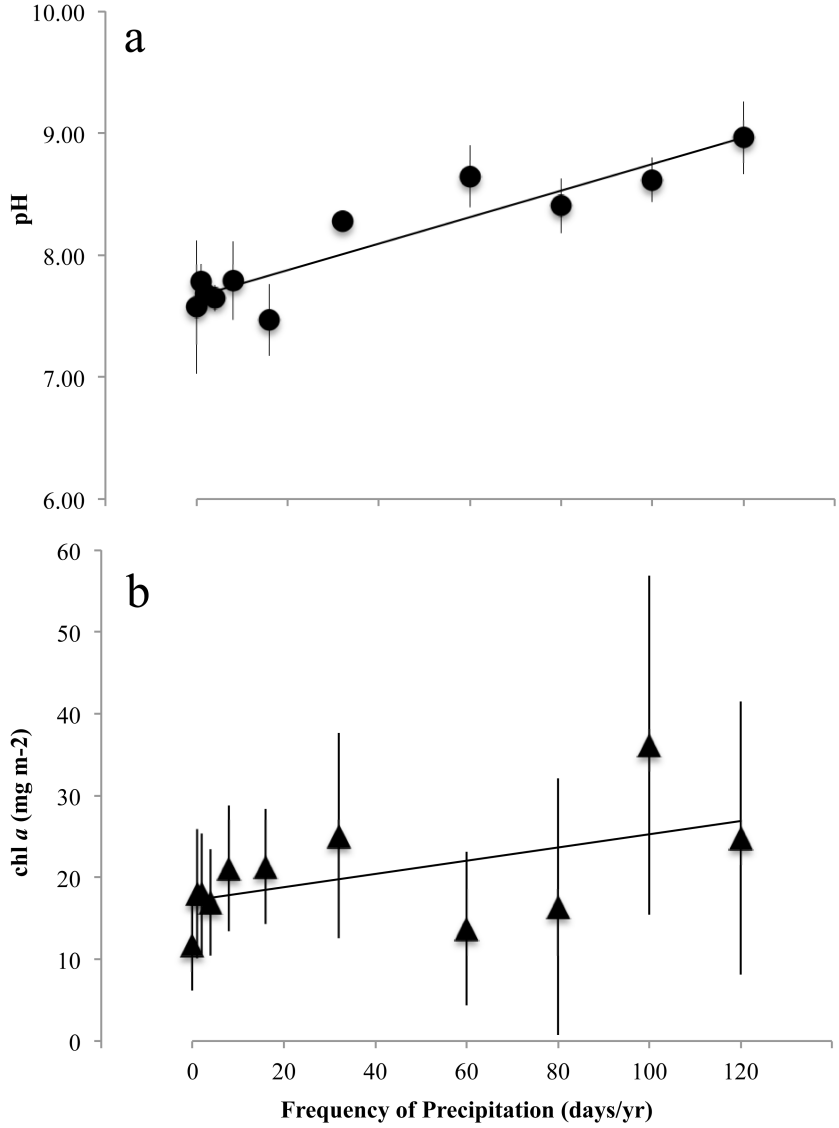

Figure 4 **Soil pH (●) and chlorophyll *a* content (▲) as a function of altered precipitation frequency treatment.** Error bars are ± std dev, lines are linear regressions.

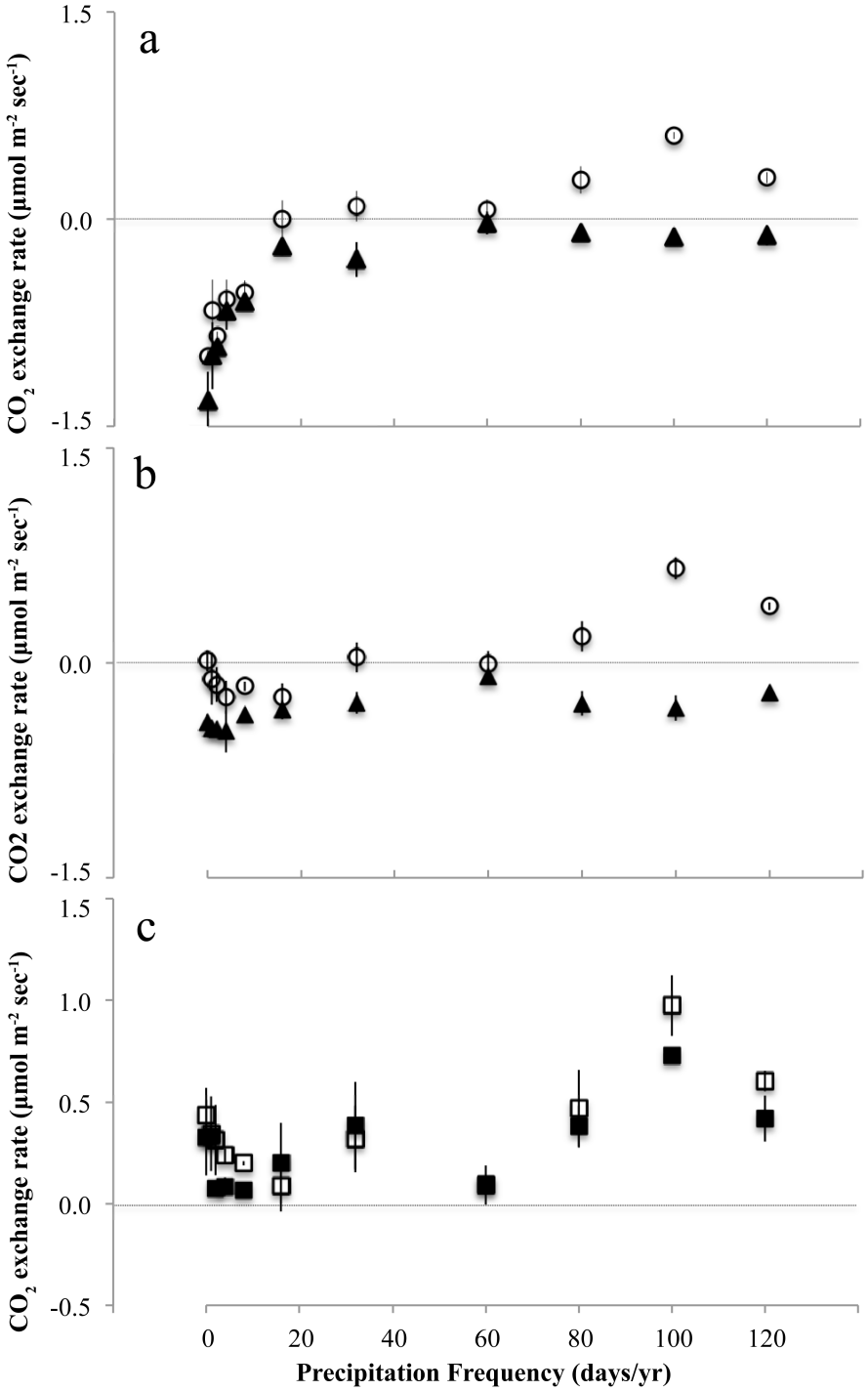

Figure 5 **Net, gross photosynthesis and respiration as a function of altered precipitation frequency. a)** Initial determination made directly after end of treatment; (○) net photosynthesis (▲) dark respiration **b)** Second measurement made 15 days after initial measurement and with 24h pre-incubation; (○) net photosynthesis (▲) dark respiration **c)** Calculated gross photosynthesis from initial determination (■) second determination (▫). Error bars are ± std dev (n=9).

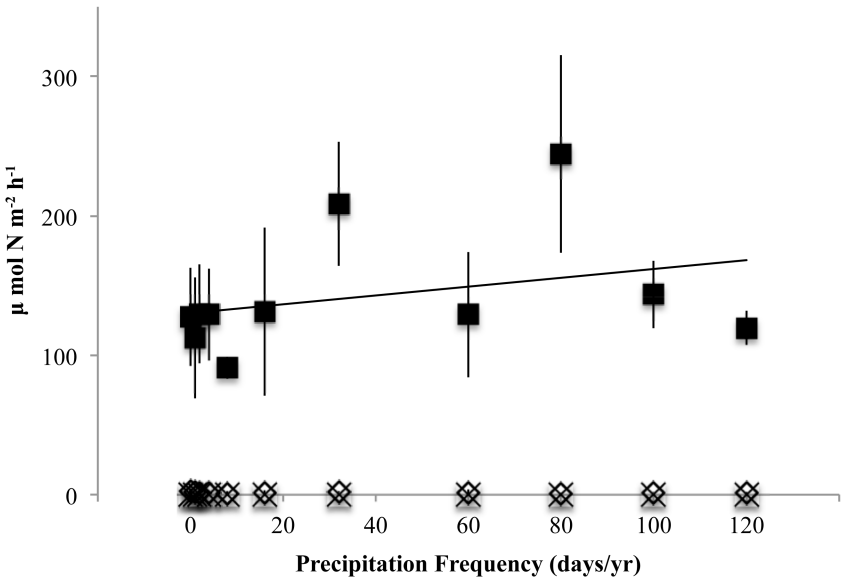

Figure 6 **Rates of nitrogen cycling as a function of altered precipitation frequency.** Error bars are ± std dev (n=3). Denitrification (◇); N-fixation (×); Ammonia oxidation(■) ($P = 0.17$, $r^2 = 0.06$)

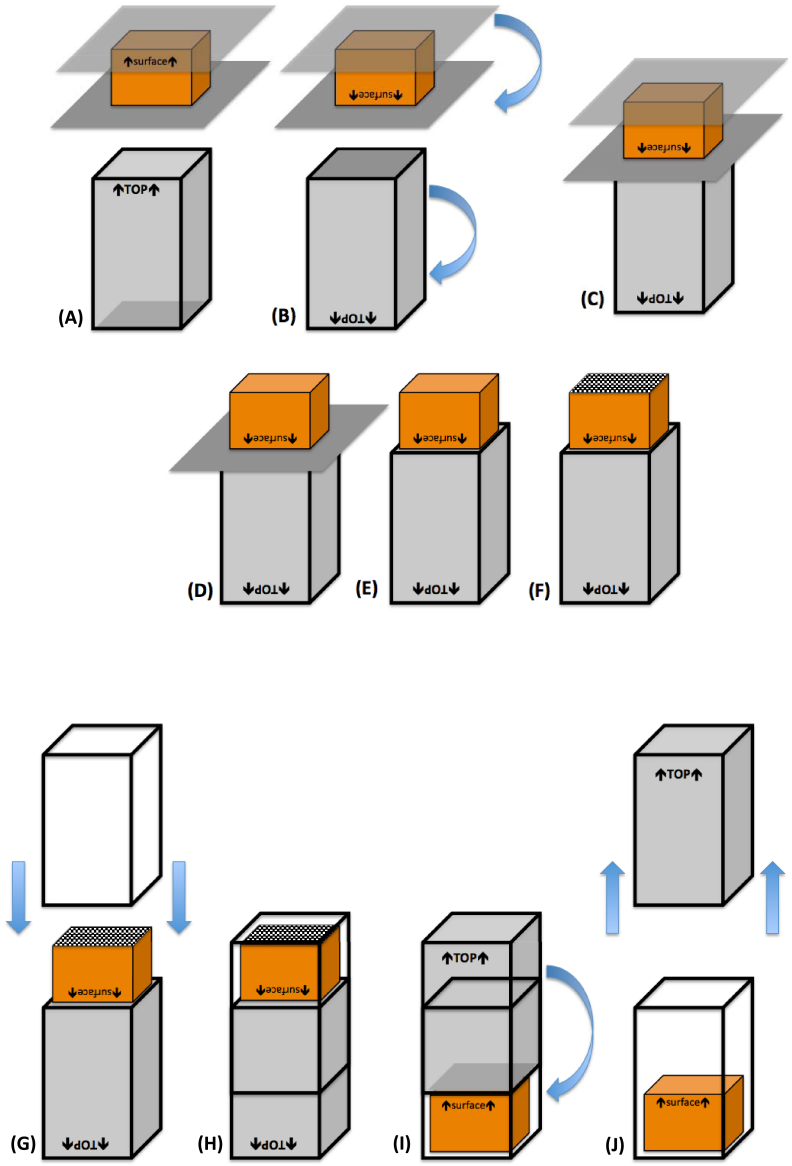

Figure S1 Microcosm construction. BSCs were cut out of the ground using a stainless steel frame, 12 cm x 12 cm x 5 cm (orange). Flat stainless steel sheets were placed under and on top of the frame (A) and the sample was inverted (B). The inverted sample was placed on top of an inverted pot (gray) (C) and the sheets were removed (D&E). A mesh screen was placed on the bottom of the sample (F) and the destination pot (clear) was inverted and placed over the sample (G&H). The nested pots were up righted (I) and the inner pot (gray) was removed (J). The frame was removed from around the crust/soil sample and the margins between the sample and pot were filled with autoclaved sand.

Precip Gradient LOW→HIGH

Frequency of Precipitation (days/yr):	0	1	2	4	8	16	32	60	80	100	120
soil slurry in Ringer's solution	0	0	0	0	0	0	0	0	0	0	0
Pyruvic Acid Methyl Ester	3	3	3	3	3	3	3	3	3	3	3
Tween 40	3	3	3	3	3	3	3	3	3	3	3
Tween 80	3	3	3	3	3	3	3	3	3	3	3
alpha-cyclodextrin	3	3	3	3	3	3	3	3	3	3	3
Glycogen	3	3	3	3	3	3	3	3	3	3	3
D-Cellobiose	3	3	3	3	3	3	3	3	3	3	2
alpha-D-Lactose	3	3	3	3	3	3	3	3	3	3	3
beta-Methyl-D-Glucoside	3	3	3	3	3	3	3	3	3	3	3
D-Xylose	3	3	3	3	3	3	3	3	3	3	3
i-Erythritol	1	3	3	2	3	2	3	3	3	3	3
D-Mannitol	3	3	3	3	3	3	3	3	3	3	3
N-Acetyl-D-Glucosamine	3	3	3	3	3	3	3	3	3	3	3
D-Glucosaminic Acid	3	3	3	3	3	3	3	3	3	3	3
Glucose-1-phosphate	0	0	1	0	1	0	0	1	1	0	0
D,L-alpha-Glycerol phosphate	2	1	2	2	1	1	3	2	2	3	2
D-Galactonic Acid gamma-Lactone	2	1	0	0	0	0	0	0	0	3	1
D-Galacturonic Acid	3	3	3	3	3	3	3	3	3	3	3
2-Hydroxy Benzoic Acid	0	0	0	0	1	0	0	2	0	0	0
4-Hydroxy Benzoic Acid	3	3	3	3	3	3	3	3	3	3	3
gamma-Hydroxybutyric Acid	3	3	3	3	3	3	3	3	3	3	3
Itaconic Acid	1	2	2	0	1	0	0	1	0	2	1
alpha-Ketobutyric Acid	3	3	3	3	3	2	3	3	3	3	3
D-Malic Acid	3	3	3	3	3	3	3	3	3	3	3
L-Arginine	3	3	3	3	3	3	3	3	3	3	3
L-Asparagine	3	3	3	3	3	3	3	3	3	3	3
L-Phenylalanine	3	3	3	3	3	3	3	3	3	3	3
L-Serine	3	3	3	3	3	3	3	3	3	3	3
L-Threonine	3	3	3	3	3	3	3	3	3	3	3
Glycyl-L-Glutamic Acid	3	3	3	3	3	3	3	3	3	3	3
Phenylethylamine	3	3	3	3	3	3	3	3	3	3	3
Putrescine	3	3	3	3	3	3	3	3	3	3	3

0 replicates  ALL replicates

Fig S2 Biolog EcoPlate Carbon Metabolism Diversity, Aerobic incubation. Carbon substrate utilization diversity at 168 h. Increasing color intensity indicates number of treatment samples (n=3) that successfully metabolized the specified carbon source. There was no correlation between carbon metabolic diversity and increasing precipitation frequency.

Precip Gradient LOW→HIGH

Frequency of Precipitation (days/yr):	0	1	2	4	8	16	32	60	80	100	120
soil slurry in Ringer's solution	0	0	0	0	0	0	0	0	0	0	0
Pyruvic Acid Methyl Ester	0	0	0	0	0	0	0	0	0	0	0
Tween 40	2	3	3	3	3	3	3	3	3	3	3
Tween 80	3	3	3	3	3	3	3	3	3	3	3
alpha-cyclodextrin	3	2	2	1	0	2	2	2	2	2	1
Glycogen	3	3	3	3	1	3	3	2	3	3	3
D-Cellobiose	3	3	3	2	1	3	2	3	3	3	3
alpha-D-Lactose	3	3	1	2	0	0	1	0	0	1	0
beta-Methyl-D-Glucoside	1	3	3	3	1	2	2	3	2	3	2
D-Xylose	0	0	0	0	0	0	0	0	0	0	0
i-Erythritol	0	0	0	0	0	0	0	0	0	0	1
D-Mannitol	2	3	2	2	0	2	1	0	1	2	1
N-Acetyl-D-Glucosamine	3	3	2	2	1	1	1	1	1	2	1
D-Glucosaminic Acid	0	0	0	0	0	0	0	0	0	0	0
Glucose-1-phosphate	0	0	0	0	0	0	0	0	0	0	0
D,L-alpha-Glycerol phosphate	0	0	0	0	0	0	0	0	0	0	0
D-Galactonic Acid gamma-Lactone	0	0	0	0	0	0	0	0	0	0	0
D-Galacturonic Acid	0	0	0	0	0	0	0	0	0	0	0
2-Hydroxy Benzoic Acid	0	0	0	0	0	0	0	0	0	0	0
4-Hydroxy Benzoic Acid	0	0	0	0	0	0	0	0	0	0	0
gamma-Hydroxybutyric Acid	0	0	0	0	0	0	0	0	0	0	0
Itaconic Acid	0	0	0	0	0	0	0	0	0	0	0
alpha-Ketobutyric Acid	0	0	0	0	0	0	0	0	0	0	0
D-Malic Acid	0	0	0	0	0	0	0	0	0	0	0
L-Arginine	0	0	0	0	0	0	0	0	0	0	0
L-Asparagine	0	0	0	0	0	0	0	0	0	0	0
L-Phenylalanine	0	0	0	0	0	0	0	0	0	0	0
L-Serine	0	0	0	0	0	0	0	0	0	0	0
L-Threonine	0	0	0	0	0	0	0	0	0	0	0
Glycyl-L-Glutamic Acid	0	0	0	0	0	0	0	0	0	0	0
Phenylethylamine	0	0	0	0	0	0	0	0	0	0	0
Putrescine	0	0	0	0	0	0	0	0	0	0	0

Fig S3 Biolog EcoPlate Carbon Metabolism Diversity, Anaerobic incubation. Carbon substrate utilization diversity at time end (168 h). Increasing color intensity indicates number of treatment samples (n=3) that successfully metabolized the specified carbon source. There was no correlation between carbon metabolic diversity and increasing precipitation frequency.